

Primordial anisotropies from cosmic strings during inflation

Sadra Jazayeri¹, Alireza Vafaei Sadr^{2,3}, Hassan Firouzjahi¹

¹*School of Astronomy, Institute for Research in Fundamental Sciences (IPM)*

P. O. Box 19395-5531, Tehran, Iran

²*Department of Physics, Shahid Beheshti University, G.C., Evin, Tehran 19839, Iran*

³*Département de Physique Théorique and Center for Astroparticle Physics, Université de Genève,
24 Quai Ernest Ansermet, 1211 Genève 4, Switzerland*

Abstract

In this work we study the imprints of a primordial cosmic string on inflationary power spectrum. Cosmic string induces two distinct contributions on curvature perturbations power spectrum. The first type of correction respects the translation invariance while violating isotropy. This generates quadrupolar statistical anisotropy in CMB maps which is constrained by the Planck data. The second contribution breaks both homogeneity and isotropy, generating a dipolar power asymmetry in variance of temperature fluctuations with its amplitude falling on small scales. We show that the strongest constraint on the tension of string is obtained from the quadrupolar anisotropy and argue that the mass scale of underlying theory responsible for the formation of string can not be much higher than the GUT scale. The predictions of string for the diagonal and off-diagonal components of CMB angular power spectrum are presented.

1 Introduction

The precise measurements of anisotropies on cosmic microwave background (CMB) temperature fluctuations and its polarization maps [1, 2, 3] have provided strong supports for inflation as the leading theory for early universe and generating the initial perturbations. The basic predictions of inflation that the CMB perturbations to be nearly scale invariant, nearly adiabatic and nearly Gaussian are well consistent with these observations.

There are indications of anomalies on CMB maps as reported in Planck results [1, 3] and also in earlier observations, such as the dipole asymmetry and the power suppressions on large scales. There are two different views as how to interpret these anomalies. One attitude is that these anomalies are not statistically significant and may be due to lack of precise data, unknown systematics or even methods of data analysis. This is mainly motivated from the fact that these anomalies are observed on low ℓ regions of CMB maps in which the effects of cosmic variance are non-negligible. It is possible that these anomalies are artifacts of poor statistics on large scales. In this view, no single anomaly is significant enough to challenge the simple concordance model of early universe. It is argued that if a theoretical model can address more than one anomalies at the same time, then these anomalies and the theory behind their generations become significant. The other attitude is that these anomalies may be genuine and may hint to non-trivial inflationary dynamics. If so, understanding these anomalies may open new window to physics of primordial universe. This is particularly important if the anomalies persist in the current and future observations. In addition, if some theoretical models can address not only anomalies in CMB temperature maps but also provide independent predictions for CMB polarization maps and primordial tensor perturbations then it worth studying these scenarios.

In particular, the Planck data indicate the existence of hemispherical power asymmetry in the CMB maps [4, 5] which was observed earlier in the WMAP data too [6, 7, 8]. Fitting the temperature anisotropy with a dipole modulation [9] in the form

$$\Delta T(\hat{\mathbf{n}}) = \overline{\Delta T(\hat{\mathbf{n}})} (1 + A_d \hat{\mathbf{n}} \cdot \hat{\mathbf{p}}) , \quad (1)$$

the Planck data found the dipole amplitude $A_d \simeq 0.06$ with the preferred direction $\hat{\mathbf{p}}$ towards the southern hemisphere with respect to the galactic plane. One interesting feature of dipole asymmetry is that the amplitude of dipole shows strong scale-dependent such that it falls off rapidly on smaller scales, say for $\ell \geq 100$. The effects of dipole asymmetry in CMB data and large scale structure have been further investigated in [10, 11, 12, 13, 14, 15, 16, 17, 18, 19, 20, 21].

With these discussions in mind there have been significant interests to address the nature of dipole asymmetry in recent years. One interesting proposal for the mechanism of dipolar asymmetry is the idea of long mode modulations [22]. In this picture it is assumed that there exists a mode k_L which is much longer than the Hubble radius during inflation. This long mode generates the power asymmetry by modulating the background inflationary parameters such as the inflaton field or its velocity or by modulating the surface of end of inflation.

Unfortunately this proposal does not work in simple models of inflation such as in single field scenarios. Based on the single field non-Gaussianity consistency condition [23], it is shown in [24] that the amplitude of dipole modulation is controlled by the amplitude of local-type non-Gaussianity f_{NL} . Consequently, in single field inflationary models with small (actually zero) f_{NL} , dipole asymmetry with large enough amplitudes can not be generated. For this idea to work, one has to consider models beyond simple slow roll scenarios such as curvaton model, iso-curvature perturbations etc. For a list of various theoretical works based on long mode modulation and related ideas to generate dipole asymmetry see [25].

Alternatively, the idea of using primordial defects during inflation to generate power asymmetry has been employed in [26] and [27]. In [26] it is assumed that there exists a domain wall during inflation which causes the asymmetry. It is shown that large dipole with non-trivial scale dependent can be generated while the amplitude of higher multipoles are suppressed as required from the Planck data. This idea was extended in [27] to the case of a primordial massive defect, such as a monopole or black hole, during inflation to generate power asymmetry. The presence of a massive defect breaks the translational invariance maximally while keeping the rotation invariance intact. The structure of power asymmetry is somewhat non-trivial as one also generates inhomogeneities in primordial power spectra.

Another anomaly which captured significant interests in recent year is quadrupolar statistical anisotropy. Unlike the hemispherical (dipolar) asymmetry defined in Eq. (1), the quadrupolar statistical anisotropy represents anisotropy at individual points. Specifically, if one divides the CMB sphere in two opposite hemispheres then both hemisphere are statistically the same while points on the same or opposite hemisphere can have different power. The quadrupolar statistical anisotropy in curvature perturbation power spectrum $P_{\mathcal{R}}$ is usually parametrized in Fourier space \mathbf{k} via [28, 29]

$$P_{\mathcal{R}}(\mathbf{k}) = P_{\mathcal{R}}^{(0)}(\mathbf{k})(1 + g_*(\hat{\mathbf{m}} \cdot \hat{\mathbf{k}})^2), \quad (2)$$

in which $P_{\mathcal{R}}^{(0)}(\mathbf{k})$ is the dominant isotropic power spectrum, $\hat{\mathbf{m}}$ represents the preferred (anisotropic) direction in the sky and g_* is the amplitude of quadrupolar anisotropy. Constraints from Planck data [30, 1, 3] implies $|g_*| \lesssim 10^{-2}$.

The best known mechanism to generate quadrupolar statistical anisotropy is the scenario of anisotropic inflation based on the dynamics of a $U(1)$ gauge field during inflation, see for example [31, 32, 33, 34, 35, 36, 37]. In this mechanism a background electric field is turned on during inflation so the background geometry is in the form of Bianchi I metric. If one couples the gauge field with the inflaton field appropriately, then one can reach the attractor regime in which the electric field energy density reaches a sub-leading but a constant fraction of the total energy density. This can leads to a small amount of quadrupole anisotropy.

Mathematically speaking, the quadrupolar statistical anisotropy given in Eq. (2) is defined in Fourier space while the hemispherical asymmetry in Eq. (1) is defined in real space. In order to prevent confusion, we refer to former as the statistical anisotropy while the latter is called power asymmetry or dipolar asymmetry.

In this work, we extend the motivation of [26, 27] to the case of a cosmic strings during inflation. Our goal is to calculate the corrections in curvature power spectrum and to look for the amplitude, shape and scale dependence of the induced anisotropy and asymmetry. The imprints of primordial defects during inflation for various motivations have been studied in [38, 39, 40, 41, 42, 43]. In particular in [39] the correction to curvature perturbation power spectrum induced by a cosmic string during inflation is obtained. In this work we build and extend on the results of [39] to obtain the imprints of a cosmic string during inflation. In the presence of a cosmic string, both of the translation and rotation invariances are partially broken while a subset of these symmetries are left intact. More specifically, the translation and the rotation along the string are still invariant. Consequently, we expect that corrections in power spectrum to retain the translation and the rotation invariances only along the string. As a result, as we shall see, cosmic string has the unique property to generate both quadrupole anisotropy and power asymmetry though with complicated shapes.

Before closing this section, we comment that independent of the observational significance of anisotropy and asymmetry, the idea of looking for the imprints of defects during inflation is well-motivated. Indeed, the formation of defect is a generic feature of symmetry breaking which are expected to happen at various scales on the history of early universe [44]. In particular, the idea of strings in early universe is interesting. In models of inflation constructed from string theory, such as in brane inflation, cosmic strings are copiously generated at the end or during inflation when a pair of brane and anti-brane annihilate each other [45, 46, 47, 48, 49, 50]. These are either fundamental strings (F-strings) or D1-branes (D-strings) which have different charges and couplings. They can combine to form junctions of (p, q) strings which can have non-trivial implications for lensing and evolution of the networks of cosmic superstrings, for a review see [51].

2 Curvature perturbations power spectrum

In this section we present our setup of a cosmic string during inflation. The motivations and the logics are similar to [26] and [27]. It is assumed that inflation is driven by a scalar field, the inflaton field ϕ , which is slowly rolling on its nearly flat potential $V(\phi)$. Therefore, the dominant source of energy density is given by the potential V . The string is assumed to be a sub-dominant source of energy and its effects can be treated perturbatively compared to those of inflaton field. We consider the idealized situation where the string's length is much larger than the Hubble radius during inflation so for practical purposes it is treated as a string with infinite length. We assume that all wiggles along the length of strings are wiped out so it can be parameterized by its tension μ . As usual, the relevant dimensionless parameter in the studies of cosmic string is the parameter $G\mu$ which measures the tension of string in units of Newton constant G . In order for our perturbative approach to be consistent and the contribution of string to energy density in a given Hubble radius H^{-1} to be sub-dominant compared to the inflaton potential, we require that $(\mu H^{-1})H^3 \ll V$ which is equivalent to

$G\mu \ll 1$. In addition, we work in the limit that the thickness of string is negligible so it can be treated as a line of distribution of energy with the tension μ .

If we consider the physical assumption that the string is formed because of a $U(1)$ symmetry breaking during inflation, then the thickness of string is related to the energy scale of symmetry breaking which is at the order $1/\sqrt{\mu}$. Therefore, assuming the thickness of string to be much smaller than the Hubble radius during inflation, we require $1/\sqrt{\mu} \ll H^{-1}$ which in turn translates into $G\mu \gg (H/M_P)^2$ in which $M_P = 1/8\pi G$ is the reduced Planck mass. Combining both conditions, we require $(H/M_P)^2 \ll G\mu \ll 1$. For typical models of inflation we expect $H/M_P \lesssim 10^{-5}$ so the above condition can be easily satisfied for $G\mu \lesssim 10^{-2}$.

The upper bound on the tension of string is $G\mu \lesssim 10^{-7}$ if a network of cosmic strings is assumed to generate parts of temperature anisotropies in CMB maps, for some recent works on this direction see for example [52, 53, 54, 55]. However, this bound does not apply to our case, since we do not consider a network of strings to generate perturbations on CMB after inflation. In our picture, we have one string in a Hubble horizon during inflation. In addition, in order not to complicate the thermal history of universe after inflation, we assume that the string is decayed to relativistic particles during reheating so all its energy goes to radiation after inflation. In general the latter assumption may not be necessary so it may be relaxed if one is interested in the presence of string after inflation.

We are interested in corrections to curvature perturbation power spectrum induced from string. Following the logics of [26, 27] the dominant contribution in comoving curvature perturbations \mathcal{R} is given by inflaton field via

$$\mathcal{R} = -\frac{H}{\dot{\phi}}\delta\phi, \quad (3)$$

in which $\delta\phi$ is the quantum fluctuations associated with the inflaton field. There are two types of contributions from string which in principle one has to take into account. First, the definition of curvature perturbation \mathcal{R} in the presence of string is modified so there will be additional term in \mathcal{R} beyond the leading term given in Eq. (3). Second, the string modifies the background geometry. As is well-known the geometry around a straight string is locally flat while it modifies the geometry globally causing a deficit angle at the order $G\mu$ around string [56]. As argued in [26, 27] the first contribution in curvature power spectrum are at the order $G\mu\sqrt{\epsilon_H}$ in which ϵ_H is the slow-roll parameter $\epsilon_H \equiv -\dot{H}/H^2$. Intuitively speaking, the first contribution comes from the gravitational back-reactions of string on inflaton dynamics which necessarily has both of small parameters $G\mu$ and $\sqrt{\epsilon_H}$. However, the second contribution is the direct contribution of string into background geometry which is at the order $G\mu$ as we calculate below. Therefore, in the slow-roll limit where $\epsilon_H \ll 1$, the leading correction is from the second contribution, i.e. the direct contribution of string in geometry. This in turn induces a correction in Hamiltonian and its effects on curvature perturbation power spectrum can be calculated using the perturbative in-in formalism [23, 57].

With these discussions in mind, now we proceed to study the effects of cosmic strings on background geometry. As mentioned before, in flat background the geometry around string

is locally flat while a deficit is induced around string. In an inflationary background with a near dS background, one expects the above picture to hold and the string only to induce a deficit angle without changing the local geometry. Specifically, assuming the infinite string is extended along the z direction, the vacuum solution of string in dS background in polar coordinate (ρ, ϕ, z) have been obtained to be [58]

$$ds^2 = -dt^2 + a(t)^2 \left(d\rho^2 + (1 - 4G\mu)^2 \rho^2 d\phi^2 + dz^2 \right), \quad (4)$$

in which $a(t) = \exp(Ht)$ is the scale factor in the dS background. To leading order in slow-roll correction we have neglected the variation of H which results in sub-leading corrections to our analysis, i.e. at the order $G\mu\sqrt{\epsilon_H}$ or higher. Note that the metric above is written non-perturbatively to all orders in $G\mu$. However, we are only interested in corrections to leading order in $G\mu$ so we shall expand the above metric to first order in $G\mu$. Also note that the above metric satisfies the intuition that the string does not change the local metric of spacetime and only induces a deficit angle equal to $8\pi G\mu$.

It is more convenient to work with the Cartesian coordinate system in which the above metric is transformed into

$$ds^2 = -dt^2 + a(t)^2 \left(d\mathbf{x}^2 - \frac{\epsilon}{\rho^2} (x^2 dy^2 + y^2 dx^2 - 2xy dx dy) \right) \quad (5)$$

in which $\rho^2 = x^2 + y^2$ and we have defined the small dimensionless parameter ϵ via

$$\epsilon = 8G\mu. \quad (6)$$

We need to calculate the interaction Hamiltonian. For this purpose, we write down the action of inflaton field in the presence of cosmic string. In our treatment the inflaton field feels the presence of string via the deformation of background geometry induced by cosmic string as given in Eq. (5). Note that in the limit where we neglect the gravitational back-reactions of string on inflaton field, we can treat the scalar field as a nearly massless scalar field with the amplitude of quantum fluctuations $H/2\pi$. The rollings of inflaton and its mass induces corrections at the order $\epsilon\sqrt{\epsilon_H}$ in anisotropic power spectrum which we neglect as mentioned before.

The action of a (nearly) massless inflaton field in the presence of cosmic string encoded in the geometry (5) is given by

$$S = -\frac{1}{2} \int d^4x \sqrt{-g} g^{\mu\nu} \partial_\mu \delta\phi \partial_\nu \delta\phi. \quad (7)$$

Calculating the inverse metric $g^{\mu\nu}$ and the determinant $\sqrt{-g}$ to leading order in ϵ , we have

$$\sqrt{-g} = a^3 \left(1 - \frac{\epsilon}{2} \right) + \mathcal{O}(\epsilon^2), \quad (8)$$

and

$$\delta g^{xx} = \epsilon \frac{y^2}{a^2 \rho^2}, \quad \delta g^{yy} = \epsilon \frac{x^2}{a^2 \rho^2}, \quad \delta g^{xy} = \delta g^{yx} = -\epsilon \frac{xy}{a^2 \rho^2}. \quad (9)$$

Since the interaction terms in the Lagrangian contain solely space derivatives, the Hamiltonian density \mathcal{H}_I simply equals the Lagrangian density $-\mathcal{L}_I$. Plugging back the above results into the action, the leading order interaction Hamiltonian is obtained to be

$$H_I = \frac{\epsilon a(t)}{2} \int d^3 \mathbf{x} \frac{(x \partial_y \delta \phi - y \partial_x \delta \phi)^2}{(x^2 + y^2)}. \quad (10)$$

Because we are interested in curvature perturbation power spectrum in Fourier space, we calculate H_I in the Fourier space, yielding

$$H_I = -\frac{a(t)\epsilon}{2(2\pi)^6} \int d^3 \mathbf{x} d^3 \mathbf{k} d^3 \mathbf{q} \frac{\delta \phi_{\mathbf{k}} \delta \phi_{\mathbf{q}}}{x^2 + y^2} (y k_x - x k_y) (y q_x - x q_y) e^{i(\mathbf{k}+\mathbf{q}) \cdot \mathbf{x}}, \quad (11)$$

in which $\delta \phi_{\mathbf{k}}$ is the amplitude of $\delta \phi$ fluctuations in Fourier space. From the above expressions for H_I we see that the system enjoys the remnant translation and rotation symmetries around the z direction, the orientation of string.

Now using the standard in-in formalism [23, 57], the corrections in two-point correlations of inflaton field induced by cosmic string to leading order in ϵ is obtained to be

$$\begin{aligned} \Delta \langle \delta \phi_{\mathbf{k}}(t_e) \delta \phi_{\mathbf{q}}(t_e) \rangle &= i \int_0^{t_e} dt' \langle [H_I(t'), \delta \phi_{\mathbf{k}} \delta \phi_{\mathbf{q}}] \rangle \\ &= -2 \text{Im} \int_0^{t_e} dt' \langle H_I(t') \delta \phi_{\mathbf{k}}(t_e) \delta \phi_{\mathbf{q}}(t_e) \rangle, \end{aligned} \quad (12)$$

in which t_e indicates the time of end of inflation.

Going to conformal time $d\eta = dt/a(t)$ we obtain

$$\begin{aligned} \Delta \langle \delta \phi_{\mathbf{k}}(t_e) \delta \phi_{\mathbf{q}}(t_e) \rangle &= 2\epsilon(2\pi) \delta(k_z + q_z) \\ &\times \int d\eta' a^2(\eta') h(\mathbf{k}_{\perp}, \mathbf{q}_{\perp}) \text{Im} \left(\delta \phi_{\mathbf{k}}(\eta') \delta \phi_{\mathbf{q}}(\eta') \delta \phi_{\mathbf{k}}^*(\eta_e) \delta \phi_{\mathbf{q}}^*(\eta_e) \right), \end{aligned} \quad (13)$$

in which \mathbf{k}_{\perp} represents the projection of \mathbf{k} on the xy plane which is perpendicular to the orientation of string and we have defined the function $h(\mathbf{k}_{\perp}, \mathbf{q}_{\perp})$ via

$$h(\mathbf{k}_{\perp}, \mathbf{q}_{\perp}) \equiv \int d^2 \mathbf{x} \frac{\exp(i(\mathbf{k} + \mathbf{q})_{\perp} \cdot \mathbf{x}_{\perp})}{x^2 + y^2} \left[x^2 q_y k_y + y^2 q_x k_x - xy(q_x k_y + q_y k_x) \right]. \quad (14)$$

One can easily check that $h(\mathbf{k}_{\perp}, \mathbf{q}_{\perp}) = h(\mathbf{q}_{\perp}, \mathbf{k}_{\perp})$. Also note that the delta function $\delta(k_z + q_z)$ in Eq. (13) is a manifestation of translation invariance along the string.

Using the following form for the wave function of inflaton field

$$\delta \phi_{\mathbf{k}} = \frac{H}{\sqrt{2k^3}} (1 - ik\eta) \exp(ik\eta),$$

the integrand in Eq. (13) simplifies to

$$2\epsilon \int_{-\infty}^0 \frac{d\eta'}{H^2 \eta'^2} \frac{H^2}{\sqrt{k^3 q^3}} \text{Im} \left[(1 - ik\eta')(1 - iq\eta') e^{i(k+q)\eta'} \right]. \quad (15)$$

Now using the relations

$$\text{Im} \int_{-\infty(1-i\epsilon)}^0 d\eta' e^{i(k+q)\eta'} = \frac{-1}{k+q} \quad (16)$$

and

$$\text{Im} \int_{-\infty(1-i\epsilon)}^0 d\eta' \left(\frac{1}{\eta'^2} - \frac{i(k+q)}{\eta'} \right) e^{i(k+q)\eta'} = -(k+q), \quad (17)$$

the integral over η' in Eq. (13) is calculated yielding

$$\begin{aligned} \Delta \langle \delta\phi_{\mathbf{k}}(t_e) \delta\phi_{\mathbf{q}}(t_e) \rangle &= \frac{\epsilon\pi H^2}{k^3 q^3} \delta(k_z + q_z) \left(\frac{kq}{k+q} - (k+q) \right) \\ &\times \left[\sum_{i \neq j} k_j q_j F_{ii}(\mathbf{k}_\perp + \mathbf{q}_\perp) - k_i q_j F_{ij}(\mathbf{k}_\perp + \mathbf{q}_\perp) \right], \end{aligned} \quad (18)$$

in which for $i, j = 1, 2$ we have defined

$$F_{ij}(\mathbf{k}_\perp) \equiv \int d^2\mathbf{x} \exp(i\mathbf{k}_\perp \cdot \mathbf{x}_\perp) \frac{x_i x_j}{x^2 + y^2}, \quad i, j = 1, 2. \quad (19)$$

With some efforts one can check that [39]

$$F_{ij}(\mathbf{k}_\perp) = 2\pi^2 \delta_{ij} \delta^2(\mathbf{k}_\perp) + \frac{4\pi}{k_1^2 + k_2^2} \left(\frac{\delta_{ij}}{2} - \frac{k_i k_j}{k_1^2 + k_2^2} \right). \quad (20)$$

Plugging the above form of $F_{ij}(\mathbf{k}_\perp)$ in Eq. (18), and noting that the curvature perturbation \mathcal{R} is related to $\delta\phi$ via $\mathcal{R} = -H\delta\phi/\dot{\phi}$, the corrections of cosmic strings in curvature perturbations two point correlation function is obtained to be

$$\begin{aligned} \Delta \langle \mathcal{R}_{\mathbf{k}}(t_e) \mathcal{R}_{\mathbf{q}}(t_e) \rangle &= -\epsilon\pi \left(\frac{H^2}{\dot{\phi}} \right)^2 \left(\frac{k^2 + q^2 + kq}{k^3 q^3 (k+q)} \right) \delta(k_z + q_z) \left[2\pi^2 \mathbf{k}_\perp \cdot \mathbf{q}_\perp \delta^2(\mathbf{k}_\perp + \mathbf{q}_\perp) \right. \\ &\quad \left. + \frac{2\pi \mathbf{k}_\perp \cdot \mathbf{q}_\perp}{(\mathbf{k}_\perp + \mathbf{q}_\perp)^2} + \frac{4\pi}{(\mathbf{k}_\perp + \mathbf{q}_\perp)^4} (k_x q_y - k_y q_x)^2 \right]. \end{aligned} \quad (21)$$

This is the main result of this section. The structure of the symmetries of two point correlation function is somewhat non-trivial. The full $SO(3)$ rotation is broken to the subset of two-dimensional rotation in the xy plane as one can easily see that all three terms above are invariant under rotation only around the string. As for translation invariance, only the first term above retains the full three-dimensional translation invariance because it has the three dimensional Dirac delta function $\delta^3(\mathbf{k} + \mathbf{q})$. The last two terms in the big bracket breaks the translation invariance in the plane perpendicular to string as they have only $\delta(k_z + q_z)$. Since the string loses the full rotation and translation invariances, its corrections in curvature perturbation power spectrum is a mixture of anisotropies and inhomogeneities. Therefore, the asymmetries generated by cosmic string is more complicated than the simple

dipole asymmetry modeled by Eq. (1) and can not be captured just by the dipole amplitude A_d .

One can check that our result for two point correlation in Eq. (21) agrees with the result obtained in [39]. Indeed, manipulating the terms inside the big bracket in Eq. (21) one can show that

$$\begin{aligned} \Delta \langle \mathcal{R}_{\mathbf{k}}(t_e) \mathcal{R}_{\mathbf{q}}(t_e) \rangle &= -\epsilon\pi \left(\frac{H^2}{\dot{\phi}} \right)^2 \left(\frac{k^2 + q^2 + kq}{k^3 q^3 (k+q)} \right) \delta(k_z + q_z) \left[2\pi^2 \mathbf{k}_\perp \cdot \mathbf{q}_\perp \delta^2(\mathbf{k}_\perp + \mathbf{q}_\perp) \right. \\ &\quad \left. - \frac{4\pi}{(\mathbf{k}_\perp + \mathbf{q}_\perp)^2} \left(\frac{\mathbf{k}_\perp \cdot \mathbf{q}_\perp}{2} - \frac{\mathbf{k}_\perp \cdot (\mathbf{k}_\perp + \mathbf{q}_\perp) \mathbf{q}_\perp \cdot (\mathbf{k}_\perp + \mathbf{q}_\perp)}{(\mathbf{k}_\perp + \mathbf{q}_\perp)^2} \right) \right], \end{aligned} \quad (22)$$

as obtained in [39].

Now adding the leading isotropic and homogenous contribution from the inflaton field itself, the total two point correlation function is given by

$$\begin{aligned} \langle \mathcal{R}_{\mathbf{k}}(t_e) \mathcal{R}_{\mathbf{q}}(t_e) \rangle &= \left(\frac{H^2}{\dot{\phi}} \right)^2 \left[\frac{(2\pi)^3}{k^3} \delta^3(\mathbf{k} + \mathbf{q}) - \epsilon\pi \left(\frac{k^2 + q^2 + kq}{k^3 q^3 (k+q)} \right) \delta(k_z + q_z) \times \right. \\ &\quad \left. \times \left[2\pi^2 \mathbf{k}_\perp \cdot \mathbf{q}_\perp \delta^2(\mathbf{k}_\perp + \mathbf{q}_\perp) + \frac{2\pi \mathbf{k}_\perp \cdot \mathbf{q}_\perp}{(\mathbf{k}_\perp + \mathbf{q}_\perp)^2} + \frac{4\pi}{(\mathbf{k}_\perp + \mathbf{q}_\perp)^4} (k_x q_y - k_y q_x)^2 \right] \right]. \end{aligned} \quad (23)$$

Having obtained the corrections from cosmic string in two point functions in Fourier space as in Eq. (21) or Eq. (22) we can use them to look for the predictions of cosmic string on the CMB temperature maps and obtain some estimations of the preferred values of the model parameters.

3 Quadrupole anisotropy

As we discussed above, the corrections in power spectrum induced from cosmic string have two distinct contributions. The first term in Eq. (21) retains the three-dimensional translation invariance while the last two terms in Eq. (21) are translation invariant only along the string.

Interestingly we see that the first term in Eq. (21) has the structure of a quadrupolar anisotropy as introduced in Eq. (2) in which the anisotropic (preferred) direction is the orientation of cosmic string. As can be seen, the contribution of quadrupolar anisotropy is quite different than the contribution of last two terms in Eq. (21) which mostly mimic a dipolar asymmetry. As we discussed before, the quadrupolar statistical anisotropy is associated with anisotropy at each point on CMB map while each CMB hemisphere has statistically the same power as the opposite hemisphere.

To calculate the amplitude of quadrupolar anisotropy g_* we compare the quadrupole term in power spectrum with the isotropic power spectrum $P_{\mathcal{R}}^{(0)}$ given by the first term in Eq. (23), obtaining

$$g_* = -\frac{3\epsilon}{8}. \quad (24)$$

The minus sign above is from the fact that $\sin^2 \theta = 1 - \cos^2 \theta$.

This is an interesting prediction. We see that cosmic string induces a quadrupole anisotropy in CMB maps which can be tested directly by cosmological observations. In particular, constraints from Planck observations [30, 1, 3] implies $|g_*| \lesssim 10^{-2}$, yielding $\epsilon \lesssim 10^{-2}$. Therefore, the scale of symmetry breaking responsible for the formation of string during inflation can not be much higher than the GUT scale. For example, if we assume that the cosmic string in early universe are in the forms of D- or F-string from string theory, then the mass scale of string theory can not be much higher than the GUT scale. In addition, we see that the sign of g_* is negative in our setup. Curiously, the sign of g_* is also negative in all known models of anisotropic inflation [37].

4 Variance of curvature perturbations

Since the last two terms in Eq. (22) are not fully homogeneous, we expect them to induce an effective power asymmetry in CMB maps. The structure of these terms are too complicated to be used directly in an analytical study. A practically useful analytical tool is to look for the variance of curvature perturbations in real space $\langle \mathcal{R}(\mathbf{x})^2 \rangle$. This provides insights about the magnitude and the form of power asymmetry generated by cosmic string in temperature fluctuations. Following the analysis of [10], Planck team has used the variance of temperature fluctuations (which is linearly related to $\mathcal{R}(\mathbf{x})$) as one of the measure of dipole asymmetry [5]. With this motivation in mind we calculate $\langle \mathcal{R}(\mathbf{x})^2 \rangle$ for our setup.

The dominant contribution in variance comes from the inflation field which is given by the usual curvature perturbation power spectrum. Denoting this dominant isotropic and homogeneous contribution by $\langle \mathcal{R}(\mathbf{x})^2 \rangle^{(0)}$, we have

$$\langle \mathcal{R}(\mathbf{x})^2 \rangle^{(0)} = \int d \ln k \left(\frac{k^3}{2\pi^2} |\mathcal{R}(\mathbf{k})|^2 \right) = \int d \ln k \mathcal{P}_{\mathcal{R}}^{(0)}, \quad (25)$$

where $\mathcal{P}_{\mathcal{R}}^{(0)}$ is the isotropic power spectrum. For single field slow roll model it is equal to $\mathcal{P}_{\mathcal{R}}^{(0)} = (H^2/2\pi\dot{\phi})^2$. Taking the power spectrum to be nearly scale invariant the variance in Eq. (25) takes the form $\langle \mathcal{R}(\mathbf{x})^2 \rangle^{(0)} = \mathcal{P}_{\mathcal{R}}^{(0)} \ln(k_S/k_L)$ in which k_L and k_S respectively are the IR and UV cutoffs of the system. Note that the logarithmic divergence is a feature of neglecting inflaton's mass. Taking into account the effects of inflation's small mass, the logarithmic divergence is expected to disappear.

The correction in variance induced by cosmic string is given by

$$\Delta \langle \mathcal{R}(\mathbf{x})^2 \rangle = \frac{1}{(2\pi)^6} \int \int d^3 \mathbf{k} d^3 \mathbf{q} e^{i(\mathbf{k}+\mathbf{q})\cdot\mathbf{x}} \Delta \langle \mathcal{R}_{\mathbf{k}} \mathcal{R}_{\mathbf{q}} \rangle, \quad (26)$$

in which $\Delta \langle \mathcal{R}_{\mathbf{k}} \mathcal{R}_{\mathbf{q}} \rangle$ is calculated in Eqs. (21) or (22). The first term in Eq. (22) is fully translation invariant so as expected it does not generate any position dependence; it only modifies the leading isotropic variance. Denoting the contribution from the first term in Eq.

(22) to variance by $\Delta\langle\mathcal{R}(\mathbf{x})^2\rangle_{\text{hom}}$. we obtain

$$\begin{aligned}\Delta\langle\mathcal{R}(\mathbf{x})^2\rangle_{\text{hom}} &= -\frac{3\epsilon}{16}\left(\frac{H}{\dot{\phi}}\right)^2\int_{-\infty}^{\infty}dk_z\int_0^{\infty}dk_{\perp}\frac{k_{\perp}^3}{(k_{\perp}^2+k_z^2)^{5/2}} \\ &= -\epsilon\int d\ln k\mathcal{P}_{\mathcal{R}}^{(0)}.\end{aligned}\quad (27)$$

As expected, this has the same structure as the leading homogeneous variance given in Eq. (25). The constraint from the quadrupole anisotropy $\epsilon \ll 1$ guarantees that the corrections in isotropic and homogeneous variance induced from the first term in (22) is sub-leading compared to contribution from inflaton field. The interesting feature is that this contribution from string has opposite sign compared to contribution from inflaton. This may be a good news to address the shortage of power on low ℓ as observed in Planck data. However, a careful data analysis must be performed to see whether the string can address the shortage of power on large scales while not changing the power on smaller scales and at the same time satisfying the constraints from the quadrupole statistical anisotropy.

The remaining two terms in Eq. (22) violates the translation invariance in xy plane and contribute nontrivially in variance. Denoting these contributions by $\Delta\langle\mathcal{R}(\mathbf{x})^2\rangle_{\text{asym}}$. we have

$$\begin{aligned}\Delta\langle\mathcal{R}(\mathbf{x})^2\rangle_{\text{asym}} &= -\epsilon\left(\frac{H^2}{\dot{\phi}}\right)^2\int\frac{d^2\mathbf{k}_{\perp}d^2\mathbf{q}_{\perp}dk_z}{(2\pi)^6}e^{i(\mathbf{k}_{\perp}+\mathbf{q}_{\perp})\cdot\mathbf{x}_{\perp}}\frac{4\pi}{(\mathbf{k}_{\perp}+\mathbf{q}_{\perp})^2}\left(\frac{k^2+q^2+kq}{k^3q^3(k+q)}\right)\Big|_{q_z=-k_z} \\ &\times\left[\frac{1}{2}\mathbf{k}_{\perp}\cdot\mathbf{q}_{\perp}-\frac{1}{(\mathbf{k}_{\perp}+\mathbf{q}_{\perp})^2}\mathbf{k}_{\perp}\cdot(\mathbf{k}_{\perp}+\mathbf{q}_{\perp})\mathbf{q}_{\perp}\cdot(\mathbf{k}_{\perp}+\mathbf{q}_{\perp})\right],\end{aligned}\quad (28)$$

in which the delta function $\delta(k_z+q_z)$ have been used to remove the integration over q_z . This also means that inside the integral we have $k=\sqrt{\mathbf{k}_{\perp}^2+k_z^2}$ and $q=\sqrt{\mathbf{q}_{\perp}^2+k_z^2}$.

Fortunately the integral over k_z can be taken analytically where

$$\int_{-\infty}^{\infty}\frac{\mathbf{k}_{\perp}^2+\mathbf{q}_{\perp}^2+2k_z^2+(\mathbf{k}_{\perp}^2+k_z^2)^{1/2}(\mathbf{q}_{\perp}^2+k_z^2)^{1/2}}{(\mathbf{k}_{\perp}^2+k_z^2)^{3/2}(\mathbf{q}_{\perp}^2+k_z^2)^{3/2}\left[(\mathbf{k}_{\perp}^2+k_z^2)^{1/2}+(\mathbf{q}_{\perp}^2+k_z^2)^{1/2}\right]}dk_z=\frac{2}{k_{\perp}^2q_{\perp}^2}.\quad (29)$$

Plugging this in Eq. (28), yields

$$\begin{aligned}\Delta\langle\mathcal{R}(\mathbf{x})^2\rangle_{\text{asym}} &= -8\pi\epsilon\left(\frac{H^2}{\dot{\phi}}\right)^2\int\frac{d^2\mathbf{k}_{\perp}d^2\mathbf{q}_{\perp}}{(2\pi)^6}\frac{e^{i(\mathbf{k}_{\perp}+\mathbf{q}_{\perp})\cdot\mathbf{x}_{\perp}}}{(\mathbf{k}_{\perp}+\mathbf{q}_{\perp})^2k_{\perp}^2q_{\perp}^2} \\ &\times\left[\frac{1}{2}\mathbf{k}_{\perp}\cdot\mathbf{q}_{\perp}-\frac{1}{(\mathbf{k}_{\perp}+\mathbf{q}_{\perp})^2}\mathbf{k}_{\perp}\cdot(\mathbf{k}_{\perp}+\mathbf{q}_{\perp})\mathbf{q}_{\perp}\cdot(\mathbf{k}_{\perp}+\mathbf{q}_{\perp})\right].\end{aligned}\quad (30)$$

The above expression for variance looks too complicated to be handled analytically. However, useful information can be obtained by looking at its asymptotic behaviors. It is easy to see that the integral above has no UV divergence as the integrand oscillate rapidly yielding a finite UV contributions. As for the IR behavior, we note that the integral is independent of scale in the sense that if we rescale all momenta and the measures by the factor $|\mathbf{x}_{\perp}|$, then the integral and the measure remain independent of scale while all scale dependents appear

at the lower cutoff of the integral, i.e. it appears at the IR cutoff of the integral. Using this insight, we rescale all momenta by $|\mathbf{x}_\perp|$ writing the asymmetric variance as

$$\begin{aligned} \Delta\langle\mathcal{R}(\mathbf{x})^2\rangle_{\text{asym.}} &= -8\pi\epsilon\left(\frac{H^2}{\dot{\phi}}\right)^2\int_{|\mathbf{k}_\perp,\mathbf{q}_\perp|>\frac{\rho}{L}}\frac{d^2\mathbf{k}_\perp d^2\mathbf{q}_\perp}{(2\pi)^6 k_\perp^2 q_\perp^2}e^{i(\mathbf{k}_\perp+\mathbf{q}_\perp)\cdot\hat{\mathbf{x}}_\perp}\frac{1}{(\mathbf{k}_\perp+\mathbf{q}_\perp)^2} \\ &\times\left[\frac{1}{2}\mathbf{k}_\perp\cdot\mathbf{q}_\perp-\frac{1}{(\mathbf{k}_\perp+\mathbf{q}_\perp)^2}\mathbf{k}_\perp\cdot(\mathbf{k}_\perp+\mathbf{q}_\perp)\mathbf{q}_\perp\cdot(\mathbf{k}_\perp+\mathbf{q}_\perp)\right]. \end{aligned} \quad (31)$$

Here $\rho\equiv x_\perp=\sqrt{x^2+y^2}$ is the perpendicular distance from the point \mathbf{x} on the CMB sphere to the string and L represents the IR comoving cutoff of the setup, the size of an imaginary box which is bigger than the observable Universe.

The scaling of the integrand above suggests that the dominant contribution in Eq. (31) comes from the IR region in which k, q approaches their IR lower end. Using this insight, we can easily obtain the order of magnitude of the above integral. For example, for the first term in big bracket above we have

$$\begin{aligned} \int\frac{d^2\mathbf{k}_\perp d^2\mathbf{q}_\perp}{k_\perp^2 q_\perp^2}\frac{\mathbf{k}_\perp\cdot\mathbf{q}_\perp}{(\mathbf{k}_\perp+\mathbf{q}_\perp)^2} &= \int d\phi_1 d\phi_2 dk_\perp dq_\perp\frac{\cos(\phi_1-\phi_2)}{k_\perp^2+q_\perp^2+2k_\perp q_\perp\cos(\phi_1-\phi_2)} \\ &\sim\int_{k_\perp,q_\perp>\frac{\rho}{L}}dk_\perp dq_\perp\frac{1}{k_\perp^2+q_\perp^2} \\ &= \frac{\pi}{2}\ln\left(\frac{\rho}{L}\right) \end{aligned} \quad (32)$$

Note that in the second line we have neglected the integrals over ϕ_1 and ϕ_2 , the angular directions of \mathbf{k}_\perp and \mathbf{q}_\perp , which do not change the IR behavior of the integral. Similarly, for the second term in big bracket in Eq. (31) we obtain

$$\int_{k_\perp,q_\perp>\frac{\rho}{L}}dk_\perp dq_\perp\frac{k_\perp q_\perp}{(k_\perp^2+q_\perp^2)^2}\simeq\frac{\pi}{2}\ln\left(\frac{\rho}{L}\right). \quad (33)$$

Combining the asymptotic results Eqs. (32) and (33) we obtain

$$\Delta\langle\mathcal{R}(\mathbf{x})^2\rangle_{\text{asym.}}\sim-\frac{\epsilon}{16\pi^3}\left(\frac{H^2}{\dot{\phi}}\right)^2\ln\left(\frac{\rho}{L}\right). \quad (34)$$

Indeed, the above result can be confirmed by taking the integral in Eq. (31) analytically. With some efforts one can take the integral over k_2 and q_2 in Eq. (31), obtaining

$$\begin{aligned} \Delta\langle\mathcal{R}(\mathbf{x})^2\rangle_{\text{asym.}} &= -\frac{\pi^3\epsilon}{(2\pi)^6}\left(\frac{H^2}{\dot{\phi}}\right)^2\int dk_1 dq_1\frac{e^{i(k_1+q_1)\rho}}{(k_1+q_1)^2} \\ &\times\left(\text{sgn}(k_1+q_1)+\text{sgn}(k_1)\right)\left(\text{sgn}(q_1)+\text{sgn}(2k_1+q_1)\right) \\ &= \frac{-\pi^3\epsilon}{(2\pi)^6}\left(\frac{H^2}{\dot{\phi}}\right)^2\int dk dq_1\frac{e^{ik\rho}}{k^2}\left(\text{sgn}(k)+\text{sgn}(k-q_1)\right)\left(\text{sgn}(q_1)+\text{sgn}(2k-q_1)\right), \end{aligned} \quad (35)$$

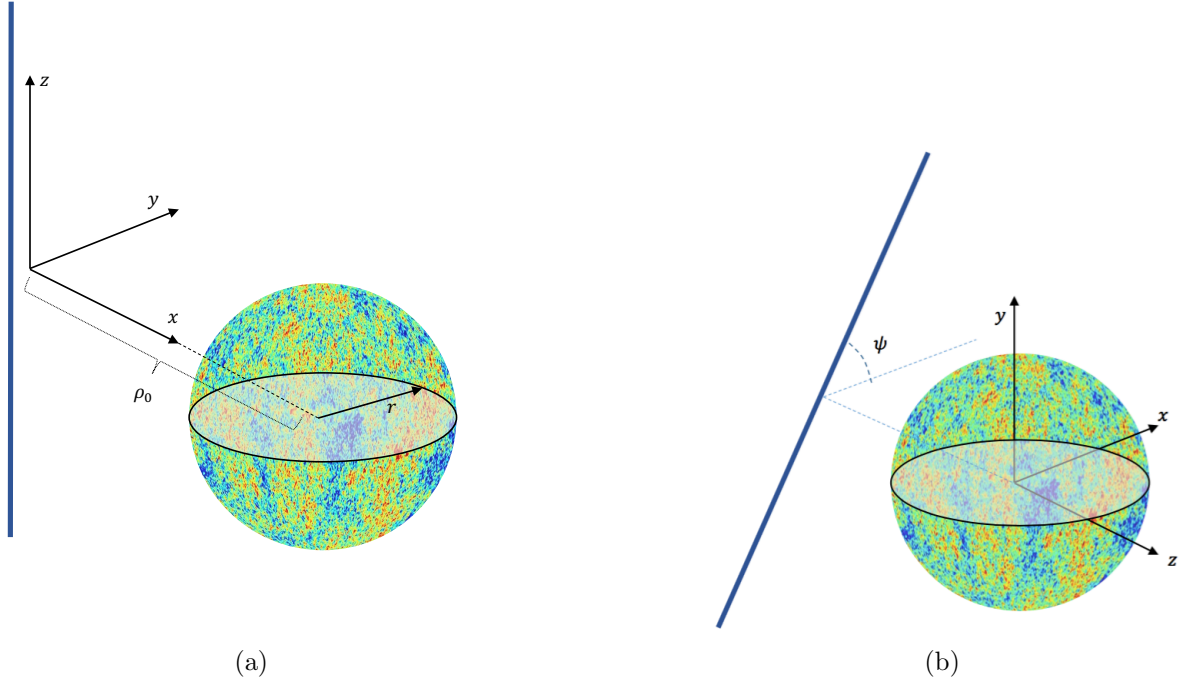


Figure 1: (a): The original coordinate system in which the string is orientated along the \hat{z} direction where we have calculated the corrections in power spectrum. (b): The new coordinate in which we perform numerical analysis for variance. The direction of dipole asymmetry is towards the $-\hat{z}$ direction. In galactic coordinate we have $\hat{z} = (l, b) = (44^\circ, 22^\circ)$ and $\hat{x} = (44^\circ, -68^\circ)$.

Taking the integral and being careful on sign functions gives the following result for the asymmetric variance

$$\begin{aligned}
 \Delta \langle \mathcal{R}(\mathbf{x})^2 \rangle_{\text{asym.}} &= -\frac{\pi^3 \epsilon}{(2\pi)^6} \left(\frac{H^2}{\dot{\phi}} \right)^2 \times 4(-2\pi^3) \text{Re} \left(\int_{\rho/L} \frac{dk}{k} \exp(ik) \right) \\
 &= -\frac{\epsilon}{8\pi^3} \left(\frac{H^2}{\dot{\phi}} \right)^2 \ln(\rho/L) \\
 &= -\frac{\epsilon}{2\pi} \mathcal{P}_{\mathcal{R}}^{(0)} \ln(\rho/L). \tag{36}
 \end{aligned}$$

Interestingly, we see that our approximate result Eq. (34) is well consistent (up to a factor of 2) with the exact result in Eq. (36).

In the next section we estimate the observational bounds on the model parameters by comparing Eq. (36) with the Planck data.

5 Numerical results and comparison with observations

Having obtained the analytical estimate for the variance of curvature perturbation in Eq. (36) in this section we look for the constraints on the model parameters by comparing our analytical result for the variance with the Planck data.

5.1 Variance of the TT map

In [10], the authors have constructed a map of variance out of the TT map of the Planck data. They have obtained the best fit values for the direction of the variance asymmetry as well as the multipole moments of the variance map. In their analysis they have assumed the $SO(2)$ symmetry for the map of the variance of temperature fluctuations. However, in our model by locating an infinite cosmic string near our Hubble patch during inflation, we have spontaneously broken all rotational symmetries as well as the two-dimensional translational group on the plane perpendicular to string. Nevertheless, in order to constrain our model's parameters with the actual data and especially with the results of [10], we average over the direction of cosmic string to resume the $SO(2)$ symmetry and thereby to compute the multipole moments of anisotropies in the map of variance.

Since we average over the orientation of string in a two-dimensional plane, the preferred direction is now the direction perpendicular to this plane. We change the coordinate system such that now the third axis is perpendicular to this plane. One particular realization of string is identified by the angle ψ measuring the angle of string with the new \hat{x} direction. For a schematic view of the orientation of string in the old and the new coordinate system look at Fig. 1.

In the new coordinate system, the anisotropic correction in variance of curvature perturbation from Eq. (36) (after removing the constant isotropic piece) is given by

$$\text{Var}(\theta, \phi | \epsilon, \kappa, \psi) = -\frac{\epsilon}{4\pi} \ln \left(1 + \kappa^2 \sin^2 \theta \sin^2(\phi - \psi) + \kappa^2 \cos^2 \theta + 2\kappa \cos \theta \right), \quad (37)$$

in which we have defined $\kappa \equiv r/\rho_0$ where ρ_0 is the distance between string and the center of CMB sphere and r is the comoving radius of CMB sphere as shown in Fig. 1. In Fig. 2 we have plotted the curves of constant variance on the CMB sphere. These curves are obtained by intersecting the hypersurfaces of constant ρ with the CMB sphere.

Now we need to average over the string direction to compute an angular spectrum for the map of variance. In order to do this, firstly we compute the a_{lm} multipoles associated with (37):

$$a_{lm} \equiv \int d\Omega Y_{lm}^*(\theta, \phi) \text{Var}(\theta, \phi). \quad (38)$$

Summing over m should give us a good measure for asymmetry. In other words, this summation removes the string direction, leaving the observer with the averaged angular power

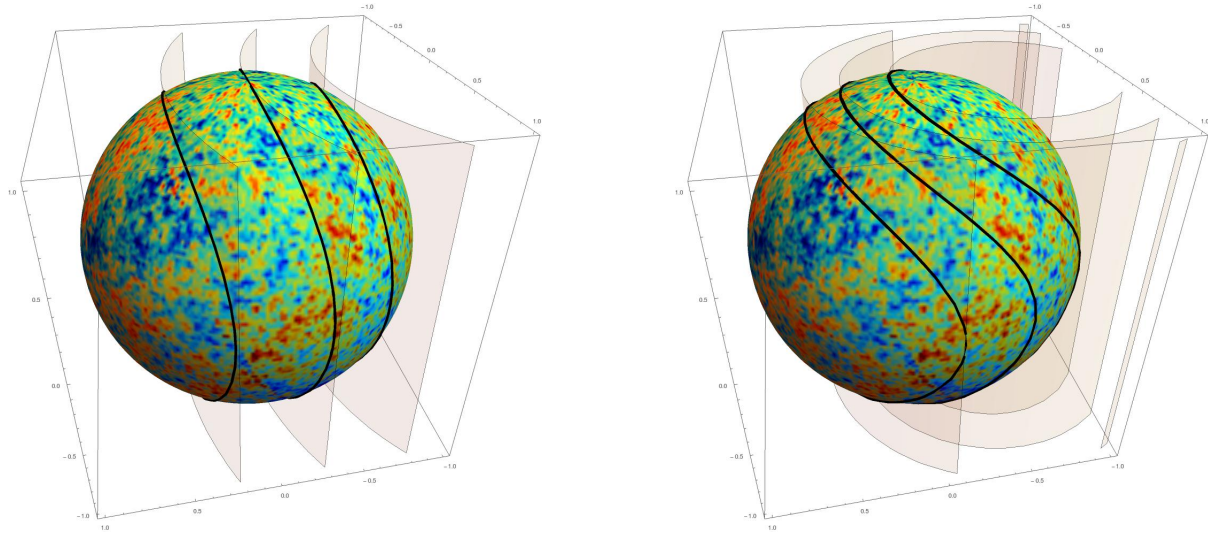


Figure 2: The curves of equal variance on CMB sphere induced by cosmic string, left: $\kappa = 0.5$, right: $\kappa = 2$. These curves are obtained by the intersection of hypersurfaces $\rho = \text{constant}$ with the CMB sphere.

spectrum

$$C_l \equiv \frac{1}{2l+1} \sum_m |a_{lm}|^2. \quad (39)$$

This is the quantity computed in [10] for both simulations and real data. In Fig. 3 we have plotted C_l for dipole, quadrupole and octupole as a function of κ .

In order to find the best fit values of our free parameters, we have rotated the Planck's map of variance of fluctuations such that the direction of the reported dipole asymmetry (in spherical coordinate) is along the $-\hat{z}$ direction, see Figs. 1 and 4. The angle of string with respect to \hat{x} in new coordinate system is represented by ψ .

Now, by means of a likelihood analysis and comparing a_{lm} with the data, one can find the best fit values for ϵ , κ and ψ . For this purpose, we used all CMB component separation algorithms, namely *Commander ruler*, *NILC*, *SMICA*, and *SEVEM* maps of Planck DR-2 intensity maps and the corresponding masks for each component [59]. We extracted variance map out of these maps by calculating the variance of the TT fluctuations over 6° circles on the CMB sphere and applied the corresponding mask for each map. Afterwards we used those disks that had more than 90 percent unmasked pixels to construct a variance map and ignored other disks. Finally, we computed a_{lm} for all of our variance maps and tried to maximize the likelihood function over the parametric space. Since a_{lm} decays rapidly for large ℓ , at the first level of analysis, we have limited ourselves to $\ell \leq 10$. Then we have found the best fit of parameters according to a pre-analysis obtained from the C_ℓ analysis like in [10]. We found that this model can not be a good fit to all C_ℓ (or a_{lm}) of the variance map. The reason is that if we try to fit high (say $\ell > 4$) multipoles simultaneously, then we miss lower multipoles

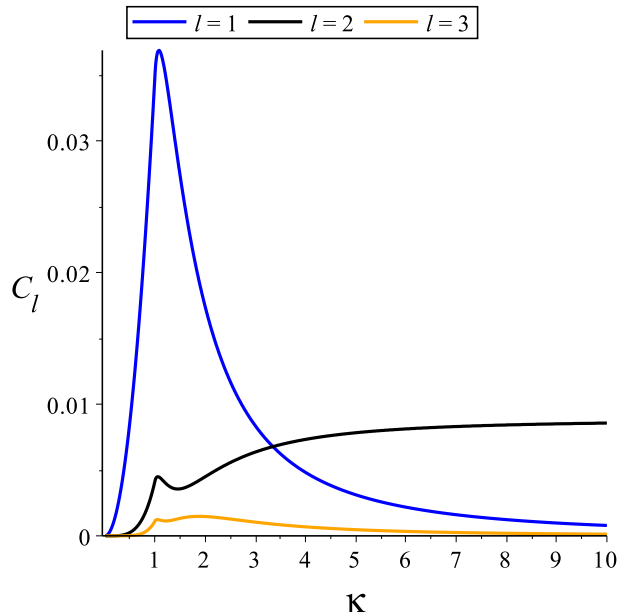


Figure 3: Angular power spectrum of the variance as a function of κ for dipole, quadrupole and octupole with the normalization $\epsilon = 1$.

and the model ceases to be a good fit to C_ℓ values for $\ell \leq 3$. Also according to [10], lower multipoles have larger confidence level compared to high ℓ values, hence when looking for the best fit values for our model's parameters, we coarse grain the variance map by looking at $\ell < 4$ multipoles. The best fit values extracted out of this procedure for our parameters are $(\epsilon, \kappa, \psi) = (0.265, 0.917, 2.518)$, see Fig. 5.

There are two important points to mention. First, we see that this best fit value, $\epsilon = 0.265$, obtained from the dipolar asymmetry is an order of magnitude weaker than the constraint $\epsilon \lesssim 10^{-2}$ obtained from the quadrupolar anisotropy. Second, the best fit value $\kappa = 0.917$ corresponds to the configuration in which the string is very close to CMB sphere. In realistic situation, it requires fine-tuning so one expects κ to be somewhat different than unity.

5.2 Angular spectrum of TT map

Here we perform the analysis of CMB angular two point function.

Computing the angular two point function of the TT map with the primordial curvature power spectrum Eq. (22) is straightforward. The details of the formulas are reported in Appendix A. It is useful to decompose the primordial spectrum into two parts as represented in Eq. (41). The first part does not violate the translational invariance and as mentioned before is simply a quadrupole term, while the second part breaks the translational invariance. These two parts have different contribution into the angular power spectrum, hence in the following we compute and plot each contribution separately.

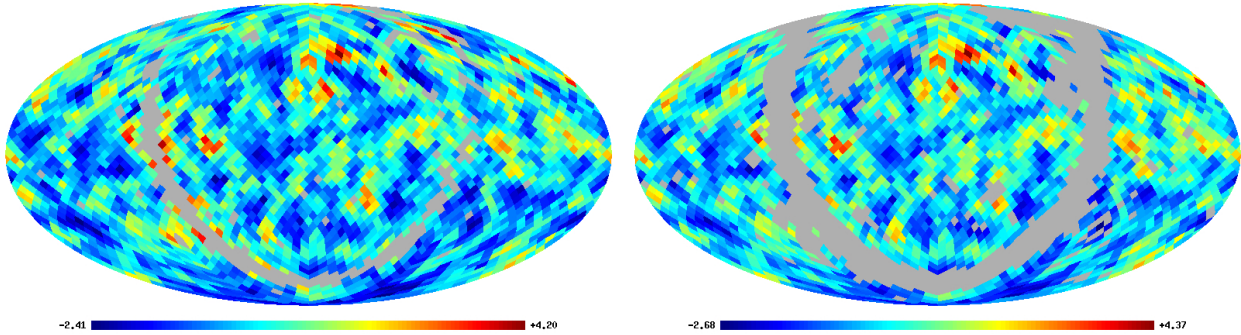


Figure 4: Left: NILC masked variance map, right: SMICA masked variance map. They are masked by their individual masks and rotated such that the vertical direction lies in the direction of dipole variance asymmetry, namely $(\ell, b) = (224, -22)$ in galactic coordinates.

The results shown in Fig. 6 are plotted for the best fit values found in Fig. 5, namely $(\epsilon, \kappa) = (0.265, 0.917)$. The second contribution which violates translation invariance rapidly decays for large ℓ s, as a result the first contribution which is homogeneous dominates over the non-homogeneous part for $\ell > 3$ for diagonal elements. We also observe that the $\ell_2 = \ell_1$ part of the second contribution is much bigger than its off-diagonal $\ell_2 = \ell_1 + 2$ elements. Computing the second contribution is numerically too expensive so we calculated only its low multipole elements.¹

6 Discussions

In this work we have looked for the imprints of a primordial cosmic string during inflation in generating statistical anisotropy and power asymmetry. The question of looking for the effects of cosmic strings in early universe is very well motivated. Cosmic strings can be generated from a $U(1)$ symmetry breaking during inflation. Alternatively, they can be the F- and D- strings of superstring theory. In either ways, constraining the tension of cosmic string directly constrains the mass scale of the corresponding underlying theories responsible for the formation of cosmic strings.

The contribution of cosmic string in curvature power spectrum has two distinct parts. The first part is homogenous and has the form of quadrupolar statistical anisotropy. Comparing with the Planck constraints on the amplitude of quadrupolar anisotropy we obtain the upper bound $G\mu \lesssim 10^{-2}$ so the energy scale of the underlying theories generating cosmic string can not be significantly higher than the GUT scale.

The second contribution of cosmic string in curvature power spectrum breaks the trans-

¹We have to keep in mind that the theoretical value for the angular power spectrum depends on coordinate we choose, due to the lack of rotational symmetry. Consequently, one can not directly compare the diagonal $C_{ll' mm'}$ terms found here with the actual C_l plots of Planck's data. Nevertheless, what we plot here should give a rough picture of how C_l would look like if we rotate our TT map in order to match the coordinate in Planck's map and if we average properly over m and m' .

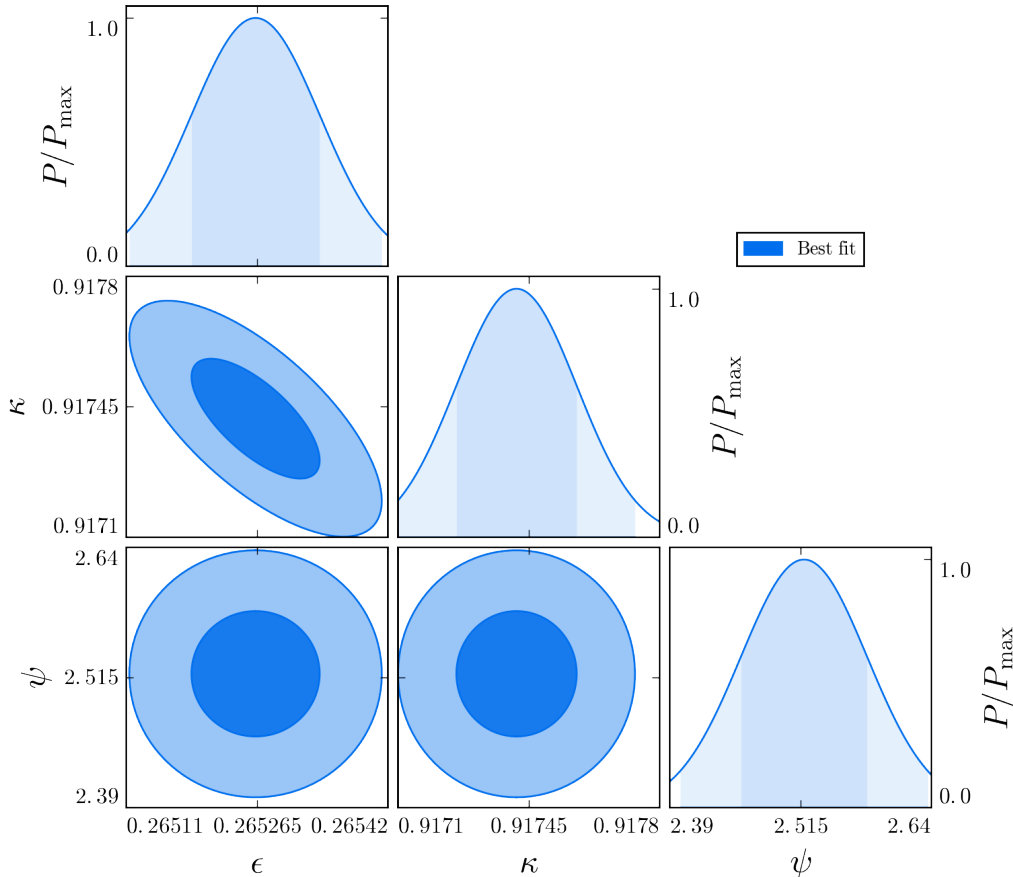


Figure 5: The three parameters Fisher analysis with the best values $(\epsilon, \kappa, \psi) = (0.265, 0.917, 2.518)$.

lation invariance in the plane perpendicular to string. This contributes to asymmetry in variance of curvature perturbations. The resulting constraint on the tension of cosmic string $G\mu \sim 10^{-1}$ is about an order of magnitude weaker than the constraint from the quadrupolar anisotropy.

We have calculated the contributions of the above mentioned two terms in CMB angular power spectrum. Because the isotropy and the homogeneities are broken, we will have off-diagonal contributions in angular power spectrum. The contribution of the inhomogeneous part rapidly falls off with ℓ for both diagonal and off-diagonal part. The non-trivial scale dependence of power asymmetry from the inhomogeneous term is a good news, as the observed dipole asymmetry in CMB maps suggest a rapid fall off for the power asymmetry in small scale. Having said this, a dedicated data analysis is required to investigate the full effects of strings on CMB temperature and polarization maps.

In our analysis we have considered the simple picture of an infinite string straight. In a realistic situation, one may encounter a network of cosmic strings during inflation. So it is an interesting question what would be the imprints of a network of cosmic strings with a mix of loops and long strings on inflationary power spectrum. During inflation the strings are

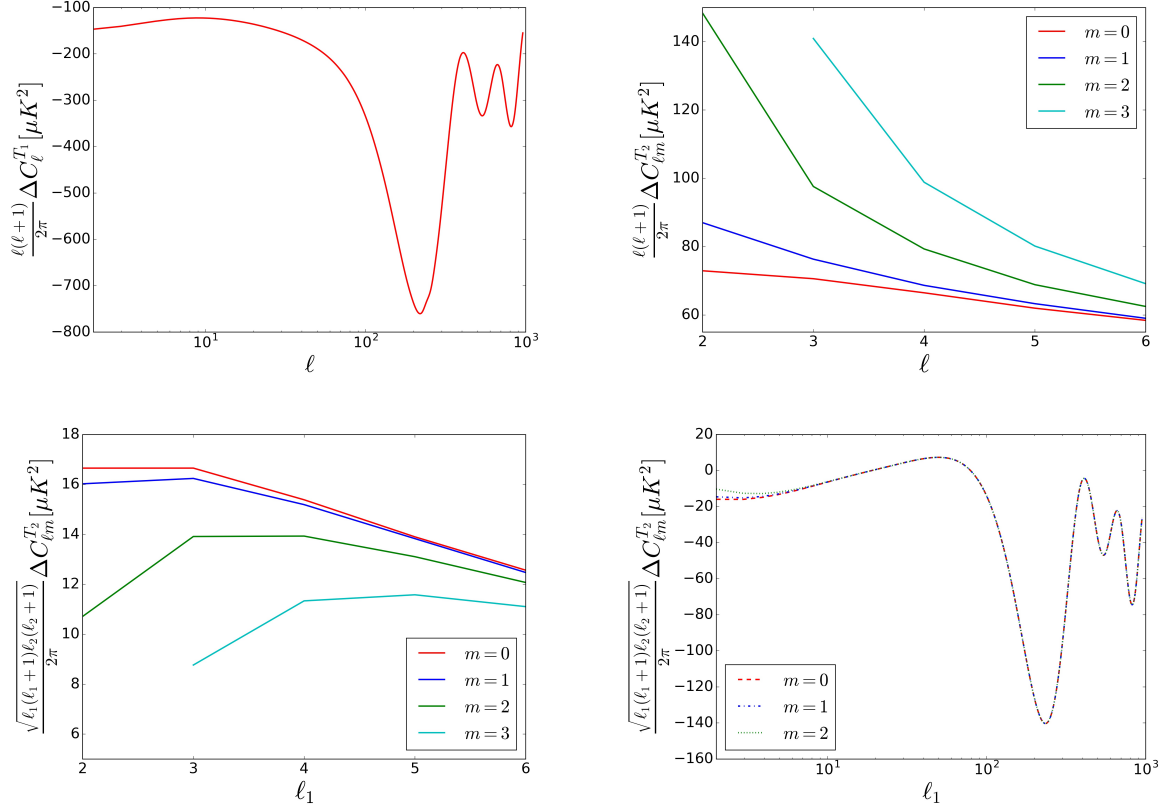


Figure 6: Some elements of the first (homogenous) and second (inhomogeneous) parts of the power spectrum Eq. (22) for the angular power spectrum matrix, $C_{(l,m)(l',m')}$, evaluated for the best fit values found by variance analysis in Fig. 5. Top left: the diagonal part of the first contribution with the sum over m . Top right: the diagonal part of the second contribution evaluated for different m . Since the computational cost of calculating this part is very high, we did not sum over all m . Lower left: the $l_2 = l_1 + 2$ elements of second part of the angular power, evaluated for different m . Lower right: the $l_2 = l_1 + 2$ element (the only non zero off diagonal element) of the first contribution for different m .

diluted quickly so if one waits for few e-folds then our picture of a long straight string is well justified. However, during the short transient regime when the strings are being diluted, the imprints of a network of cosmic strings in inflationary power spectrum would be much more complicated than our results. It may be an interesting question to look for the transient effects of a network of cosmic string during early stage of inflation and to see whether a network of cosmic strings can address the anomalies on CMB maps.

Acknowledgments: We thank Yashar Akrami, Jaume Garriga, Martin Kunz and Alessio Notari for useful discussions. H. F. would like to thank the University of Barcelona for hospitality where this work was at its final stage. The computations were performed at

University of Geneva on the Baobab cluster.

A Angular power spectrum

The relation between the primordial curvature perturbations and angular fluctuations of the CMB is given by

$$a_{lm} = 4\pi i^l \int \frac{d^3k}{(2\pi)^3} \Delta_l(k) \mathcal{R}_{\mathbf{k}} Y_{lm}(\hat{k}), \quad (40)$$

where $\mathcal{R}_{\mathbf{k}}$ is the curvature perturbations of a particular mode.

As discussed in the main text the corrections from cosmic string in power spectrum, given in Eq. (22), have two distinct parts:

$$\Delta \langle \mathcal{R}_{\mathbf{k}} \mathcal{R}_{\mathbf{q}}^* \rangle = \mathcal{F}_1(\mathbf{k}) \delta^3(\mathbf{k} - \mathbf{q}) + \mathcal{F}_2(\mathbf{k}_{\perp}, \mathbf{q}_{\perp}) \delta(k_z - q_z). \quad (41)$$

The term \mathcal{F}_1 violates the isotropy but not the homogeneity, while \mathcal{F}_2 violates both isotropy and homogeneity. These functions are given by the following formulas:

$$\begin{aligned} \mathcal{F}_1(\mathbf{k}) &= 12\pi^5 \epsilon \mathcal{P}_{\mathcal{R}}^{(0)} \frac{\sin^2 \theta}{k^3} \\ \mathcal{F}_2(\mathbf{k}_{\perp}, \mathbf{q}_{\perp}) &= -(2\pi)^4 \epsilon \mathcal{P}_{\mathcal{R}}^{(0)} \frac{\exp(i(k_1 - q_1)\rho)}{k^3 q^3} \left(\frac{k^2 + q^2 + kq}{k + q} \right) \\ &\quad \frac{1}{(\mathbf{k}_{\perp} - \mathbf{q}_{\perp})^2} \left\{ \frac{1}{2} \mathbf{k}_{\perp} \cdot \mathbf{q}_{\perp} - \frac{1}{(\mathbf{k}_{\perp} - \mathbf{q}_{\perp})^2} \mathbf{k}_{\perp} \cdot (\mathbf{k}_{\perp} - \mathbf{q}_{\perp}) \mathbf{q}_{\perp} \cdot (\mathbf{k}_{\perp} - \mathbf{q}_{\perp}) \right\}. \end{aligned} \quad (42)$$

The matrix elements of the TT anisotropies are ²

$$C_{(l,m)(l',m')}^{TT} = \langle a_{lm} a_{l'm'}^* \rangle = (4\pi)^2 i^{l-l'} \int \frac{d^3k d^3q}{(2\pi)^6} \Delta_l(k) \Delta_{l'}(q) Y_{lm}(\hat{k}) Y_{l'm'}^*(\hat{q}) \langle \mathcal{R}_{\mathbf{k}} \mathcal{R}_{\mathbf{q}}^* \rangle. \quad (43)$$

We separate the matrix elements due to different terms in (41). The first piece contributes as

$$C_{(l,m)(l',m')}^I = (4\pi)^2 i^{l-l'} \int \frac{d^3k}{(2\pi)^6} \Delta_l(k) \Delta_{l'}(k) \mathcal{F}_1(\mathbf{k}) Y_{lm}(\hat{k}) Y_{l'm'}^*(\hat{k}). \quad (44)$$

Hereafter the following convention for spherical harmonics functions is being used:

$$Y_{lm}(\theta, \phi) = \sqrt{\frac{(2l+1)(l-m)!}{4\pi(l+m)!}} P_l^m(\cos \theta) \exp(im\phi). \quad (45)$$

Correspondingly, Eq. (44) simplifies to

$$\begin{aligned} C_{(l,m)(l',m')}^I &= \delta_{mm'} \sqrt{(2l+1) \frac{(l-m)!}{(l+m)!}} \sqrt{(2l'+1) \frac{(l'-m)!}{(l'+m)!}} (4\pi) i^{l-l'} \\ &\quad \times \int \frac{k^2 dk \sin \theta d\theta}{(2\pi)^5} \Delta_l(k) \Delta_{l'}(k) \mathcal{F}_1(k, \theta) P_l^m(\cos \theta) P_{l'}^{m*}(\cos \theta). \end{aligned} \quad (46)$$

²Note that a_{lm} depends on the coordinate system we work with as shown in Fig. 1.

As for the second term we have:

$$C_{(l,m)(l'm')}^{II} = (4\pi)^2 i^{l-l'} \int \frac{k^2 dk d\phi \sin \theta d\theta}{(2\pi)^6} Q dQ d\phi' \Delta_l(k) \Delta_{l'}(\sqrt{Q^2 + k^2 \cos^2 \theta}) \quad (47)$$

$$\times Y_{lm}(\cos \theta, \phi) Y_{l'm'}^*\left(\frac{k \cos \theta}{\sqrt{Q^2 + k^2 \cos^2 \theta}}, \phi'\right) \mathcal{F}_2(\mathbf{k}_\perp, \mathbf{q}_\perp).$$

These expressions are used in our analysis to calculate the angular power spectrum in generating plots in Fig. 6.

References

- [1] P. A. R. Ade *et al.* [Planck Collaboration], *Astron. Astrophys.* **594**, A20 (2016).
- [2] P. A. R. Ade *et al.* [Planck Collaboration], *Astron. Astrophys.* **594**, A13 (2016).
- [3] P. A. R. Ade *et al.* [Planck Collaboration], *Astron. Astrophys.* **571**, A22 (2014)
- [4] P. A. R. Ade *et al.* [Planck Collaboration], *Astron. Astrophys.* **571**, A23 (2014).
- [5] P. A. R. Ade *et al.* [Planck Collaboration], *Astron. Astrophys.* **594**, A16 (2016) .
- [6] H. K. Eriksen, F. K. Hansen, A. J. Banday, K. M. Gorski and P. B. Lilje, *Astrophys. J.* **605**, 14 (2004), [Erratum-*ibid.* **609**, 1198 (2004)].
- [7] H. K. Eriksen, G. Huey, R. Saha, F. K. Hansen, J. Dick, A. J. Banday, K. M. Gorski and P. Jain *et al.*, *Astrophys. J.* **656**, 641 (2007) .
- [8] H. K. Eriksen, A. J. Banday, K. M. Gorski, F. K. Hansen and P. B. Lilje, *Astrophys. J.* **660**, L81 (2007).
- [9] C. Gordon, W. Hu, D. Huterer and T. M. Crawford, *Phys. Rev. D* **72**, 103002 (2005) .
- [10] Y. Akrami, Y. Fantaye, A. Shafieloo, H. K. Eriksen, F. K. Hansen, A. J. Banday and K. M. Gorski, *Astrophys. J.* **784**, L42 (2014) .
- [11] S. Aiola, B. Wang, A. Kosowsky, T. Kahniashvili and H. Firouzjahi, *Phys. Rev. D* **92**, 063008 (2015) .
- [12] S. Mukherjee, P. K. Aluri, S. Das, S. Shaikh and T. Souradeep, *JCAP* **1606**, no. 06, 042 (2016).
- [13] S. Mukherjee and T. Souradeep, *Phys. Rev. Lett.* **116**, no. 22, 221301 (2016) .
- [14] S. Adhikari, *Mon. Not. Roy. Astron. Soc.* **446**, no. 4, 4232 (2015) .

- [15] M. Quartin and A. Notari, JCAP **1501**, no. 01, 008 (2015).
A. Notari, M. Quartin and R. Catena, JCAP **1403**, 019 (2014).
O. Roldan, A. Notari and M. Quartin, JCAP **1606**, no. 06, 026 (2016).
- [16] M. Shiraishi, N. S. Sugiyama and T. Okumura, Phys. Rev. D **95**, no. 6, 063508 (2017).
- [17] M. Shiraishi, J. B. Muoz, M. Kamionkowski and A. Raccanelli, Phys. Rev. D **93**, no. 10, 103506 (2016).
- [18] S. Baghram, A. A. Abolhasani, H. Firouzjahi and M. H. Namjoo, JCAP **1412**, no. 12, 036 (2014).
- [19] F. Hassani, S. Baghram and H. Firouzjahi, JCAP **1605**, no. 05, 044 (2016).
- [20] J. P. Zibin and D. Contreras, arXiv:1512.02618 [astro-ph.CO].
- [21] S. Yasini and E. Pierpaoli, arXiv:1610.00015 [astro-ph.CO].
- [22] A. L. Erickcek, M. Kamionkowski and S. M. Carroll, Phys. Rev. D **78**, 123520 (2008) .
A. L. Erickcek, S. M. Carroll and M. Kamionkowski, Phys. Rev. D **78**, 083012 (2008) .
A. L. Erickcek, C. M. Hirata and M. Kamionkowski, Phys. Rev. D **80**, 083507 (2009) .
L. Dai, D. Jeong, M. Kamionkowski and J. Chluba, Phys. Rev. D **87**, 123005 (2013) .
- [23] J. M. Maldacena, JHEP **0305**, 013 (2003).
- [24] M. H. Namjoo, S. Baghram and H. Firouzjahi, Phys. Rev. D **88**, 083527 (2013);
A. A. Abolhasani, S. Baghram, H. Firouzjahi and M. H. Namjoo, Phys. Rev. D **89**, no. 6, 063511 (2014);
M. H. Namjoo, A. A. Abolhasani, S. Baghram and H. Firouzjahi, JCAP **1408**, 002 (2014).
- [25] D. H. Lyth, JCAP **1308**, 007 (2013).
J. F. Donoghue, K. Dutta and A. Ross, Phys. Rev. D **80**, 023526 (2009).
L. Wang and A. Mazumdar, Phys. Rev. D **88**, 023512 (2013).
A. Mazumdar and L. Wang, JCAP **1310**, 049 (2013).
M. H. Namjoo, A. A. Abolhasani, H. Assadullahi, S. Baghram, H. Firouzjahi and D. Wands, JCAP **1505**, no. 05, 015 (2015).
H. Assadullahi, H. Firouzjahi, M. H. Namjoo and D. Wands, JCAP **1504**, no. 04, 017 (2015).
H. Firouzjahi, J. O. Gong and M. H. Namjoo, JCAP **1411**, no. 11, 037 (2014).
M. Zarei, Eur. Phys. J. C **75**, no. 6, 268 (2015).

- J. McDonald, JCAP **1307**, 043 (2013).
- J. McDonald, JCAP **1311**, 041 (2013).
- J. McDonald, Phys. Rev. D **89**, 127303 (2014).
- S. Kanno, M. Sasaki and T. Tanaka, PTEP **2013**, no. 11, 111E01 (2013).
- A. R. Liddle and M. Cortes, Phys. Rev. Lett. **111**, 111302 (2013).
- T. Kobayashi, M. Cores and A. R. Liddle, JCAP **1505**, no. 05, 029 (2015).
- G. D’Amico, R. Gobbetti, M. Kleban and M. Schillo, JCAP **1311**, 013 (2013).
- Z. -G. Liu, Z. -K. Guo and Y. -S. Piao, Phys. Rev. D **88**, 063539 (2013).
- Z. G. Liu, Z. K. Guo and Y. S. Piao, Eur. Phys. J. C **74**, no. 8, 3006 (2014).
- Y. F. Cai, W. Zhao and Y. Zhang, Phys. Rev. D **89**, no. 2, 023005 (2014)
- Z. Chang, X. Li and S. Wang, Chin. Phys. C **39**, no. 5, 055101 (2015).
- K. Kohri, C. M. Lin and T. Matsuda, JCAP **1408**, 026 (2014).
- Z. Chang and S. Wang, arXiv:1312.6575 [astro-ph.CO].
- Z. Kenton, D. J. Mulryne and S. Thomas, Phys. Rev. D **92**, 023505 (2015).
- S. Mukherjee, Phys. Rev. D **91**, no. 6, 062002 (2015).
- A. Ashoorioon and T. Koivisto, Phys. Rev. D **94**, no. 4, 043009 (2016).
- S. Adhikari, S. Shandera and A. L. Erickcek, Phys. Rev. D **93**, no. 2, 023524 (2016).
- C. T. Byrnes, D. Regan, D. Seery and E. R. M. Tarrant, JCAP **1606**, no. 06, 025 (2016).
- C. T. Byrnes and E. R. M. Tarrant, JCAP **1507**, 007 (2015).
- C. T. Byrnes, D. Regan, D. Seery and E. R. M. Tarrant, Phys. Rev. D **93**, no. 12, 123003 (2016).
- C. Byrnes, G. Domenech, M. Sasaki and T. Takahashi, JCAP **1612**, no. 12, 020 (2016).
- [26] S. Jazayeri, Y. Akrami, H. Firouzjahi, A. R. Solomon and Y. Wang, JCAP **1411**, 044 (2014).
- [27] H. Firouzjahi, A. Karami and T. Rostami, JCAP **1610**, no. 10, 023 (2016).
- [28] L. Ackerman, S. M. Carroll and M. B. Wise, Phys. Rev. D **75**, 083502 (2007); Erratum: [Phys. Rev. D **80**, 069901 (2009)].
- [29] A. R. Pullen and M. Kamionkowski, Phys. Rev. D **76**, 103529 (2007).
- [30] J. Kim and E. Komatsu, Phys. Rev. D **88**, 101301 (2013).
- [31] M. a. Watanabe, S. Kanno and J. Soda, Phys. Rev. Lett. **102**, 191302 (2009).
- [32] M. a. Watanabe, S. Kanno and J. Soda, Prog. Theor. Phys. **123**, 1041 (2010).

- [33] N. Bartolo, S. Matarrese, M. Peloso and A. Ricciardone, *Phys. Rev. D* **87**, 023504 (2013).
- [34] M. Shiraishi, E. Komatsu, M. Peloso and N. Barnaby, *JCAP* **1305**, 002 (2013).
- [35] R. Emami, arXiv:1511.01683 [astro-ph.CO].
- [36] A. A. Abolhasani, R. Emami, J. T. Firouzjaee and H. Firouzjahi, *JCAP* **1308**, 016 (2013).
- [37] T. Rostami, A. Karami and H. Firouzjahi, arXiv:1702.03744 [astro-ph.CO].
- [38] S. M. Carroll, C. Y. Tseng and M. B. Wise, *Phys. Rev. D* **81**, 083501 (2010).
- [39] C. Y. Tseng and M. B. Wise, *Phys. Rev. D* **80**, 103512 (2009).
- [40] T. Prokopec and P. Reska, *JCAP* **1103**, 050 (2011).
- [41] C. H. Wang, Y. H. Wu and S. D. H. Hsu, *Phys. Lett. B* **713**, 6 (2012).
- [42] H. T. Cho, K. W. Ng and I. C. Wang, *Class. Quant. Grav.* **28**, 055004 (2011).
- [43] H. T. Cho, K. W. Ng and I. C. Wang, *JCAP* **1411**, no. 11, 023 (2014).
- [44] T. W. B. Kibble, *J. Phys. A* **9**, 1387 (1976).
- [45] S. Sarangi and S. H. H. Tye, *Phys. Lett. B* **536**, 185 (2002).
- [46] N. T. Jones, H. Stoica and S. H. H. Tye, *Phys. Lett. B* **563**, 6 (2003).
- [47] E. J. Copeland, R. C. Myers and J. Polchinski, *JHEP* **0406**, 013 (2004).
- [48] H. Firouzjahi and S.-H. H. Tye, *JCAP* **0503**, 009 (2005).
- [49] H. Firouzjahi, L. Leblond and S.-H. Henry Tye, *JHEP* **0605**, 047 (2006).
- [50] D. F. Chernoff and S.-H. H. Tye, *Int. J. Mod. Phys. D* **24**, no. 03, 1530010 (2015).
- [51] S.-H. Henry Tye, *Lect. Notes Phys.* **737**, 949 (2008).
- [52] J. Lizarraga, J. Urrestilla, D. Daverio, M. Hindmarsh and M. Kunz, *JCAP* **1610**, no. 10, 042 (2016).
- [53] T. Charnock, A. Avgoustidis, E. J. Copeland and A. Moss, *Phys. Rev. D* **93**, no. 12, 123503 (2016).
- [54] J. Lizarraga, J. Urrestilla, D. Daverio, M. Hindmarsh, M. Kunz and A. R. Liddle, *Phys. Rev. D* **90**, no. 10, 103504 (2014).
- [55] A. Lazanu and P. Shellard, *JCAP* **1502**, no. 02, 024 (2015).

- [56] A. Vilenkin and E. P. S. Shellard, “Cosmic Strings and Other Topological Defects.”
- [57] S. Weinberg, Phys. Rev. D **72**, 043514 (2005).
- [58] A. H. Abbassi, A. M. Abbassi and H. Razmi, Phys. Rev. D **67**, 103504 (2003)
- [59] R. Adam *et al.* [Planck Collaboration], Astron. Astrophys. **594**, A9 (2016).